De novo design of peptides that form transmembrane barrel pores killing antibiotic resistant bacteria

Rahul Deb[1,2,3], Ivo Kabelka[1], Jan Přibyl[1] and Robert Vácha[1,3,4]*

[1]CEITEC − Central European Institute of Technology, Masaryk University, Kamenice 5, 62500 Brno, Czech Republic;
[2]Biomolecular Chemistry and Bioinformatics, Faculty of Science, Masaryk University, Kamenice 5, 62500 Brno, Czech Republic;
[3]National Centre for Biomolecular Research, Faculty of Science, Masaryk University, Kamenice 5, 62500 Brno, Czech Republic;
[4]Department of Condensed Matter Physics, Faculty of Science, Masaryk University, Kotlářská 2, 61137 Brno, Czech Republic.
*Corresponding author. Email: robert.vacha@mail.muni.cz

De novo design of peptides that self-assemble into transmembrane barrel-like nanopores is challenging due to the complexity of several competing interactions involving peptides, lipids, water, and ions. Here, we develop a computational approach for the *de novo* design of α-helical peptides that self-assemble into stable transmembrane barrel pores with a central nano-sized functional channel. We formulate the previously missing design guidelines and report 52 sequence patterns that can be tuned for specific applications using the identified role of each residue. Atomic force microscopy, fluorescent dye leakage, and cryo-EM experiments confirm that the designed peptides form leaky membrane nanopores *in vitro*. Customized designed peptides act as antimicrobial agents able to kill even antibiotic-resistant ESKAPE bacteria at micromolar concentrations, while exhibiting low toxicity to human cells. The peptides and their assembled nanopore structures can be similarly fine-tuned for other medical and biotechnological applications.

The *de novo* design of protein sequences that fold and spontaneously assemble into a target structure with the desired function is a crucial test of our current knowledge about protein self-assembly and the ability to develop protein-based tools. Designed protein tools include small peptides, which can modulate the permeability of biological membranes by self-assembling into functional nano-sized transmembrane barrel pores (TBPs), i.e., transmembrane peptide bundles with a central channel/pore of a few nanometers width, capable of conducting water/ions and small molecules across the lipid membranes (Fig. 1a). These TBPs have applications in both biotechnology and medicine[1,2], including antimicrobial peptides (AMPs)[3]. Pore-forming AMPs can directly kill bacteria, including multidrug-resistant strains, by rapid permeabilization of bacterial membranes, and bacteria develop resistance slowly against such AMPs[4], suggesting that these peptides could become the next-generation antibiotics[5]. However, despite discovery of thousands of AMPs, alamethicin remains the only known natural AMP which was conclusively shown to form TBP[6].

De novo design of TBP-forming peptides is challenging because of the number of competing interactions that determine the stability of pore structure in the lipid membranes. Peptide-peptide interactions, which are necessary to stabilize TBP, compete with peptide-membrane and peptide-water/ion interactions. Due to such complex environment, the self-assembled pores have been shown to be highly sensitive to peptide amino acid composition, with a single-residue mutation capable of destabilizing the pore structure[7]. There are a few examples of *de novo* designed helical structures similar to TBPs (e.g., narrow ion channels or double-barrel pores)[8–12] and redesigned naturally-occurring channel-containing proteins[13–15]. However, the generalized design principles are still missing, and the role of individual residues in these structures remains either unknown or involved in specific tight-packing interactions, restricting the introduction of possible mutations for different applications. Experimental determination of residue role is challenging because it requires high spatial and temporal resolution of potentially metastable nanostructures[16]. Computer simulations can provide the required atomic resolution and add the details of interaction energies for such dynamic structures[7,17].

Here, we perform molecular dynamics (MD) simulations to determine the role of amino acids at each sequence position for the stabilization of large TBPs. Based on the simulation results, we formulate the so far missing design guidelines and propose a set of sequence patterns for α-helical peptides that are able to form stable TBPs with a central water channel. Provided guidelines enable custom design of self-assembled peptide nanopores tunable for specific functions. We use the obtained knowledge to *de novo* design pore-forming potent AMPs that are capable of selectively killing pathogenic Gram-positive and Gram-negative bacteria while sparing human cells, suggesting their potential antibiotic functions, and implying that the peptides can be similarly tuned for a wide range of applications.

Computer simulations

To analyze the role of each peptide residue in TBP stabilization/destabilization, we designed 144 model peptides with systematically modified sequences, and tested the ability of each peptide to stabilize the TBP over a 51 μs long unbiased MD simulation using coarse-grained

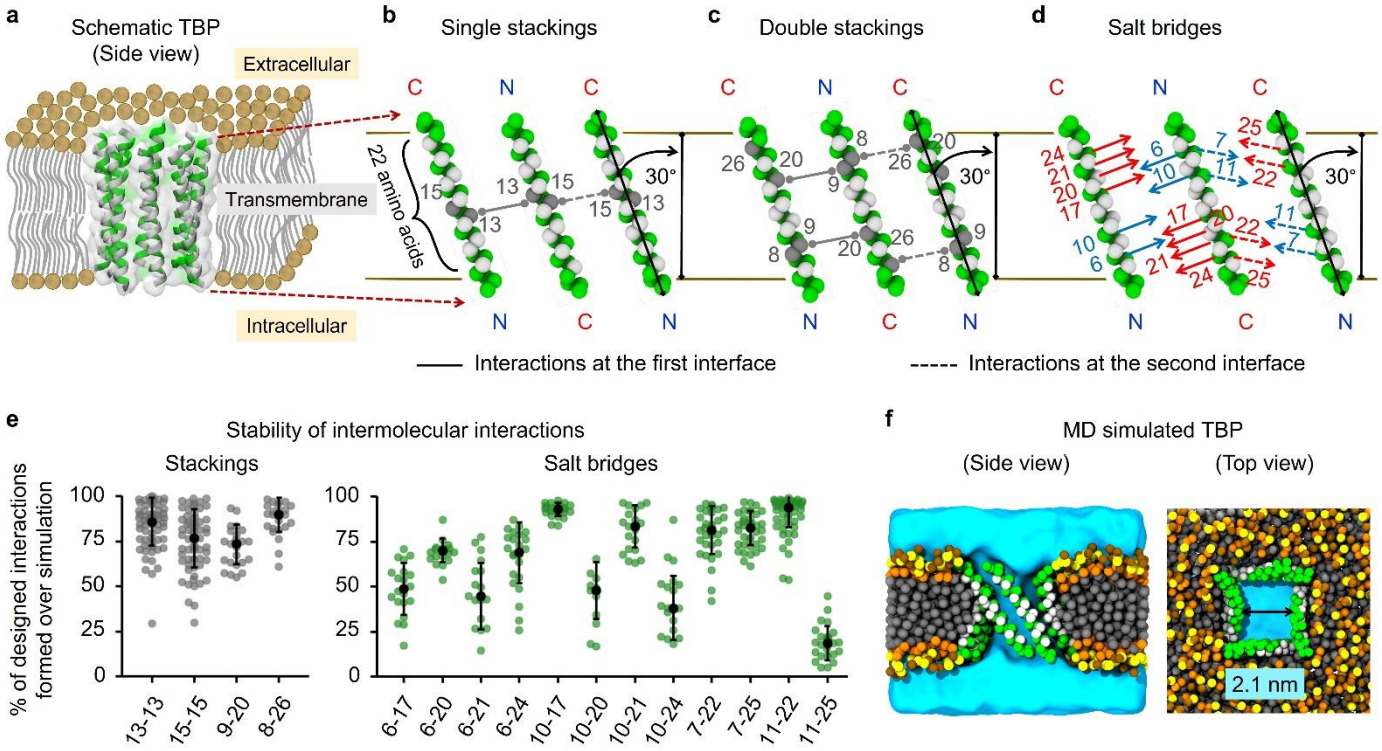

Fig. 1 | Computational design of α-helical TBP. a, Schematic representation of an octameric TBP formed by α-helical (ribbons) peptides made of 30 amino acids. **b-d,** Illustration of the antiparallel transmembrane peptide arrangements (tilted by 30° with respect to the membrane normal due to the peptide hydrophobic patches made of ~22 residues) with two representative peptide-peptide interfaces indicating the simulation-suggested optimal positions for residues forming pore-stabilizing intermolecular interactions: (b) single and (c) double π-π stacking between aromatic hydrophobic residues (gray) per interface, and (d) salt bridges between cationic (blue) and anionic (red) residues. Horizontal lines demarcate the membrane lipid headgroups. **e,** Stability of the intermolecular stacking and salt bridge interactions between the investigated residue pairs in TBPs. For an individual residue pair, each point represents the percentage of designed/intended interactions that formed over the simulation run. **f,** Simulation snapshots (taken after 51 μs) depicting the water channel (blue) of ~2 nm diameter inside an octameric TBP stabilized by the designed RDFA2 peptides (Supplementary Table 3) in POPC membrane, which is represented by CG beads showing lipid cholines, phosphates, glycerols and tails in ochre, yellow, orange and silver colors, respectively. Peptides are represented by their backbone CG beads colored green and white for hydrophilic and hydrophobic residues, respectively.

(CG) Martini force field[18] (see methods in Supplementary information for details). We assumed that the peptides would spontaneously assemble into a TBP structure once that becomes the lowest energy state stabilized via strong peptide-peptide interactions. We focused on amphipathic α-helical peptides composed of 30 amino acids, an approximate helix length required to span the thickness of a common model membrane made of 1-palmitoyl-2-oleoyl-*sn*-glycero-3-phosphocholine (POPC) lipids[19]. We chose to design single-ring octameric TBPs, the smallest nanopore structure to allow the passage of organic molecules bigger than water/ions[11], and selected an antiparallel peptide arrangement, which is favored over the parallel arrangement in helix self-assembly[17,19], see Fig 1a.

To investigate the pore-stabilizing effects of hydrophobic residues, we studied peptides composed of non-polar leucine (L) and isoleucine (I), aromatic tryptophan (W) and phenylalanine (F), and polar glutamine (Q), asparagine (N) amino acids (Supplementary Table 1). Our simulations demonstrated that the peptides, composed of LIQN residues, could not stabilize octameric TBPs, regardless of their different hydrophobicities, unless the peptide-peptide interactions were enhanced via inclusion of aromatic residues (Supplementary Fig. 1 and Table 2). Detailed analysis revealed that aromatic residues needed to be in specific positions to promote the formation of TBP-stabilizing intermolecular π-π stacking interactions (Supplementary Fig. 2). Aromatic residues at other positions could lead to intramolecular stacking, which did not stabilize TBPs (Supplementary texts). The optimal positions for residues forming intermolecular interactions depend on transmembrane peptide tilt in the pore, which is determined by the hydrophobic mismatch between the membrane hydrophobic core and the peptide hydrophobic patch[17,19]. With hydrophilic termini and the membrane hydrophobic core-spanning ~22 residue-long hydrophobic patch[8], peptides adopted a tilt of 30° in TBP and the

identified optimal positions were 13 and 15 for a single stacking and 8, 9, 20, and 26 for double stacking interactions on each peptide-peptide interface (Fig. 1b-c, Supplementary Figs. 3-4, and Supplementary texts). Hydrophilic peptide termini (outside the membrane hydrophobic core) can be modified for different purposes, e.g., oppositely charged termini can stabilize TBPs via electrostatic interactions and cationic termini can stabilize the transmembrane orientation of peptides in TBPs (Supplementary texts) and also enhance a peptide's selectivity for bacteria over human cells[20].

To analyze TBP stabilization by additional salt bridge interactions on the polar face of the peptides, we tested various combinations of oppositely charged arginine (R) and aspartic acid (D) amino acids (Fig. 1d). Peptides were designed with either 2 (groups A and B) or 4 (groups C and D) salt bridges on each peptide-peptide interface in the TBP (Supplementary Tables 3-4 and Supplementary texts). Simulations revealed that the stability of the designed/intended intermolecular salt bridge interactions increased according to their positions as follows: 10-24 < 10-20 ≈ 6-21 < 6-17 < 6-24 < 6-20 < 10-21 < 10-17 on the first interface, and 11-25 < 7-22 < 7-25 < 11-22 on the second interface (Fig. 1e). We also identified the positions at which charged residues formed unintended intermolecular salt bridges imparting additional stability to TBPs, as well as the positions at which residues formed unintended intramolecular salt bridges, which decreased the stability of the intended interactions (Supplementary Fig. 5, Table 5, and Supplementary texts). In general, the peptides from groups C and D stabilized TBPs more than the peptides from groups A and B, due to the formation of an extended ladder of interfacial salt bridge interactions, known as the electrostatic "charge zipper"[21]. Octameric TBPs with such charge zipper interactions remained stable even after several mutations and/or system modifications, including: (i) R-to-K (lysine) substitutions and/or increased peptide net charge; (ii) switching the positions of charged residues forming a salt bridge pair; (iii) substituting polar and non-polar residues to a wide variety of amino acids, including threonine (T), serine (S), alanine (A), methionine (M), valine (V), and glutamic acid (E); (iv) removal of the aromatic π-π stacking interactions; (v) using a modified 'scaled' Martini force field; and (vi) using a simple mimic of bacterial membranes composed of zwitterionic 1-palmitoyl-2-oleoyl-*sn*-glycero-3-phosphoethanolamine (POPE) and anionic 1-palmitoyl-2-oleoyl-*sn*-glycero-3-phospho-1′-rac-glycerol (POPG) lipids (3:1 mol/mol)[22], see Supplementary Figs. 6-10, Tables 6-16, and Supplementary texts for details. Free energy calculations revealed that stronger electrostatic attraction between anionic POPE:POPG membrane and cationic peptides resulted in an enhanced membrane affinity compared to zwitterionic POPC membrane, suggesting bacterial cell selectivity (Supplementary Fig. 10).

The simulated structures of our *de novo* designed TBPs (Fig. 1f) are reminiscent of the ion channels formed by prototypical alamethicin[23] and $(LSSLLSL)_3$ peptides[8]. However, our designed TBPs have larger diameter (~2.1 nm) and transmembrane peptide tilt, antiparallel peptide arrangements, and optimized stacking and salt bridge interactions (Supplementary Fig. 11 and Supplementary texts). As anticipated, our pore-stabilizing peptides spontaneously formed TBPs from the initial membrane surface-adsorbed states, with the following self-assembly process: (i) initial insertion of one peptide into the transmembrane state, (ii) transmembrane insertion of more peptide(s), (iii) formation of a water channel across the lipid membrane, (iv) oligomerization of the transmembrane peptides, and (v) system relaxation into a regular TBP with large internal cavity and a continuous water channel (Supplementary Fig. 12 and Table 17). However, the TBP formation was stochastic over the limited (simulation) time-scales and was facilitated by initially placing peptides near to the membrane hydrophobic core (Supplementary Fig. 13 and Supplementary texts).

Design guidelines

Based on our *in silico* findings, we developed a set of guidelines for the rational design of α-helical peptides that are able to self-assemble into stable, nano-sized TBPs with an antiparallel peptide arrangement. The guidelines generated 8 primary sequence templates with the identified role of each residue (Fig. 2), leading to a set of 52 sequence patterns which are organized in four groups A, B, C and D, and summarized in Supplementary Table 18. The design guidelines are as follows:

1) The proposed TBP-forming peptides are initially made of 30 amino acids, with a helical amphipathic character spanning ~ 22 amino acids in the middle of the sequence, i.e., having a continuous hydrophobic patch in an α-helical conformation.

2) Polar amino acids forming the hydrophilic patch include T, Q, S, and N. Non-polar amino acids forming the hydrophobic patch include A, M, V, L, and I. Peptides made of amino acids with high polarity (Q and N) and hydrophobicity (L and I) are preferred for pore stability.

3) Oppositely charged amino acids (cationic R and K, anionic D and E) within the hydrophilic patch are designed to form intermolecular salt bridge interactions. Either two (groups A and B) or four salt bridges (groups C and D) can be designed on each peptide-peptide interface. TBPs designed with two salt bridges per interface require further stabilization via interactions involving aromatic residues or between peptide termini. Pairs of positions at which the oppositely charged residues form salt bridge interactions

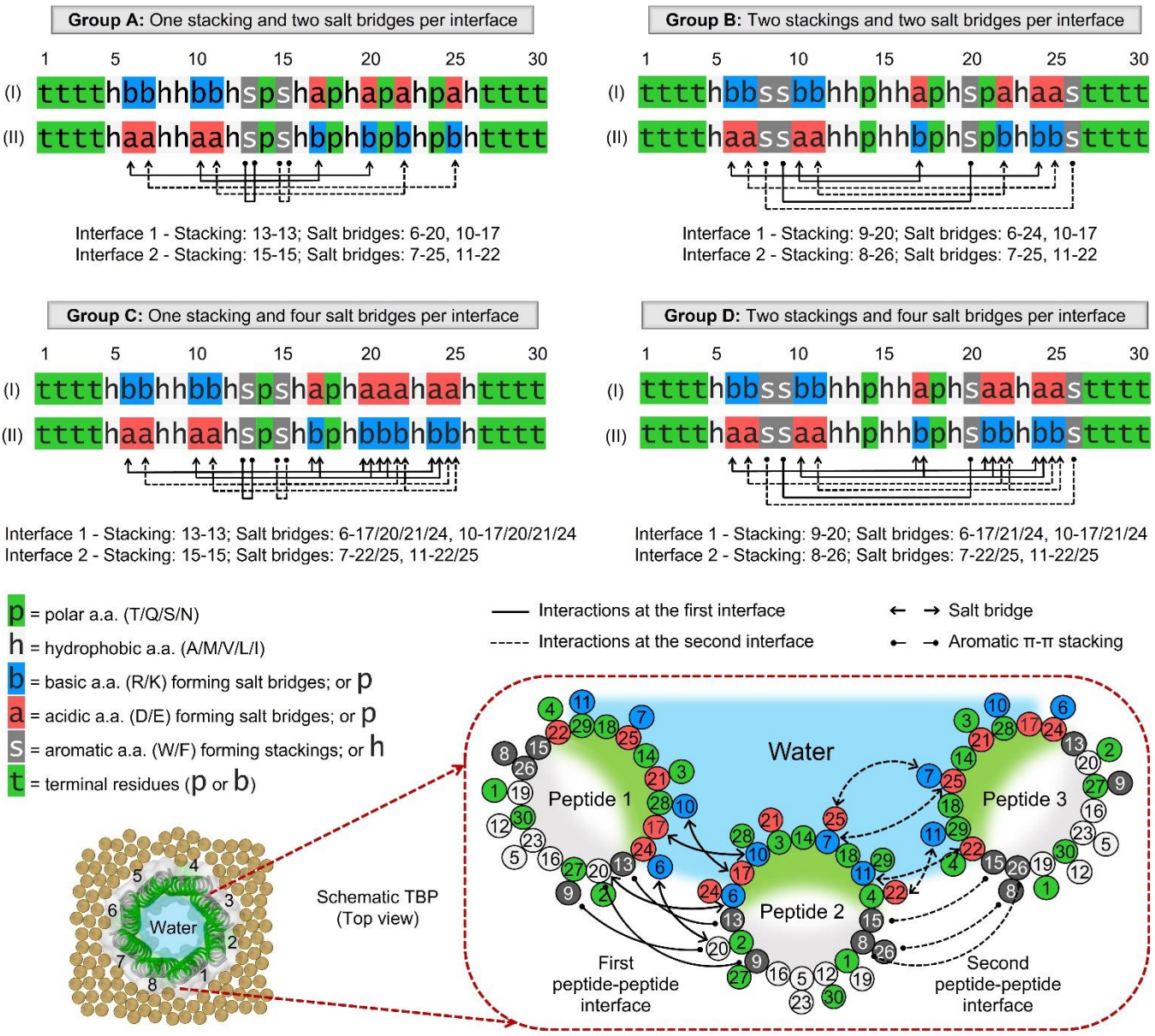

Fig. 2 | Design guidelines for α-helical peptides able to self-assemble into stable, nano-sized TBPs. Top, Eight primary sequence templates of length 30 amino acids (a.a.) (with the hydrophobic patches spanning over ~22 residues) are categorized into four groups (A, B, C, D) based on the total number of stacking and salt bridge interactions designed on each peptide-peptide interface in the TBP. Two templates (I and II), proposed for each group, have switched positions of the charged residues forming salt bridge pairs. Stability of the salt bridge interactions is as follows: 10-24 < 10-20 ≈ 6-21 < 6-17 < 6-24 < 6-20 < 10-21 < 10-17 on the first interface, and 11-25 < 7-22 < 7-25 < 11-22 on the second interface. **Bottom,** Illustration of the most stable salt bridge and stacking interactions between three antiparallel transmembrane peptides (left: helical ribbons, right: helical wheels) with two representative interfaces from an octameric TBP. Color coding: peptide hydrophilic and hydrophobic patches in green and white, respectively; membrane lipid heads in ochre; and water in blue.

are as follows - Group A: 6-20 or 10-17 on the first interface, and 7-25 or 11-22 on the second interface; Group B: 6-24 or 10-17 on the first interface, and 7-25 or 11-22 on the second interface; Groups C and D: the first salt bridge pair chosen from 6-17, 6-20, 6-21, or 6-24, and the second salt bridge pair chosen from 10-17, 10-20, 10-21 or 10-24 for the first interface, and the first salt bridge pair chosen from 7-22 or 7-25, and the second salt bridge pair chosen from 11-22 or 11-25 for the second interface. Each residue should be involved only in one salt bridge interaction. Overall, the stability of salt bridge pairs increases in the following order: 10-24 < 10-20 ≈ 6-21 < 6-17 < 6-24 < 6-20 < 10-21 < 10-17 on the first interface, and 11-25 < 7-22 < 7-25 < 11-22 on the second interface.

4) Aromatic non-polar amino acids (W and F) within the hydrophobic patch are designed to form intermolecular aromatic π-π stacking interactions. Optimal positions are 13 and 15 for a single stacking on each peptide-peptide

interface (groups A and C), and 8, 9, 20, and 26 for dual stackings on each interface (groups B and D).

5) Four residues at each peptide terminus are kept polar and can be modified for different applications. If the peptide termini are made charged, electrostatic and salt bridge interactions between the oppositely charged termini of the neighboring antiparallel transmembrane peptides can further stabilize TBPs. Furthermore, cationic residues at the termini help to stabilize the transmembrane orientation of peptides in TBP. However, in case of peptides designed with two salt bridges per interface (groups A and B), the inclusion of such charged residues can alter the stability of designed interactions due to the formation of unintended inter- and/or intramolecular salt bridges. Therefore, the oppositely charged residues should not be combined at the following positions: 6-2/3, 7-3/4, 24-27, and 25-28/29. Note that peptide length can be adjusted for specific functions by extending or shortening both the polar termini.

We corroborated these guidelines in simulations with designed negative control peptides of similar amino acid compositions, but without pore-stabilizing interactions (see Supplementary Table 19 and Supplementary texts for details).

Experimental validations

To validate the guidelines, we synthesized and *in vitro* characterized 24 designed peptides (Supplementary Table 20). Seventeen of these 24 peptides were soluble in PBS buffer and 14 peptides caused concentration-dependent leakage (efflux) of the fluorescent dye calcein from POPC:POPG (1:1 mol/mol) large unilamellar vesicles (LUVs), a simple mimic of bacterial membranes, indicating membrane nanopore formation (Fig. 3a and Supplementary Fig. 14A). Eleven peptides caused >50% leakage at a peptide/lipid (P:L) ratio of 1:100 (mol/mol) and the most active peptide, KDFA2i+9-NH2, caused ~90% leakage. Consistent with our simulations, the vesicle-permeabilizing abilities of our designed peptides were retained in the absence of aromatic stacking interactions, with the switched positions of residues forming SB pairs, in the presence of intramolecular salt bridges, and with a variety of amino acids (see Supplementary texts for details). The only exception was the SV-variant peptide KDFC16+9SV-NH2, where the resultant TBP likely has a channel too narrow for the dye leakage, because of the tight-packing of luminal S residues[24]. Two negative control peptides did not permeabilize LUVs. Seven insoluble peptides caused occasional leakage after partial dissolution via vigorous vortexing (Supplementary Fig. 14B). These peptides have low net charge (+4e) and R clusters with a propensity for aggregation[25].

Twelve of the 14 vesicle-permeabilizing peptides demonstrated antimicrobial activity (<50 μM) against at least one of the two tested model bacterial strains (Gram-negative *Escherichia coli* and Gram-positive *Staphylococcus carnosus*) and 9 soluble peptides (including the SV-variant) showed bactericidal activity against both strains (Fig. 3b, Supplementary Figs. 15-16 and Table 20). Two vesicle-permeabilizing peptides that were not active against bacteria have low net charge (+4e). We found that increasing peptide net charge (to +9e) and/or R-to-K substitutions led to higher activity, in agreement with the previous reports[26,27] (Supplementary texts). Against *E. coli*, KDFA2i+9-NH2 and KDFC16+9-NH2 had the highest activity with a minimum inhibitory concentration (MIC) of 0.8 μM, which is 15 times lower than the reference antibiotic ampicillin. Against *S. carnosus*, the most effective peptides were KDFC16+9-NH2 and KDFC16+9SV-NH2 with a MIC of 0.4 μM, which is 4 times higher than ampicillin. Only 1 of the 17 soluble peptides (RDFA2i+9-NH2, the R-variant of KDFA2i+9-NH2) showed toxicity below 50 μM against human red blood cells (HRBCs) with the 50% inhibitory concentration (IC_{50}) of 0.9 μM, which is comparable to the reference hemolytic peptide melittin[28] (Fig. 3c and Supplementary Fig. 17). Five tested potent peptides exhibited toxicity against human dermal fibroblasts (HDFs) at concentrations which were considerably above the bacterial MIC values (Fig. 3c and Supplementary Fig. 18). Peptide toxicity was reduced after R-to-K substitutions, probably due to weaker interactions with the common phospholipids that are present in human plasma membrane[26] (Supplementary texts).

The highly active AMP KDFA2i+9-NH2, with therapeutic indices of $TI_{(HRBCs\text{-}bacteria)}$ >63 and $TI_{(HDFs\text{-}bacteria)}$ ~121, also showed activity against the antibiotic-resistant ESKAPE pathogens, including *Klebsiella pneumoniae*, *Acinetobacter baumannii*, and *E. coli*, with MICs of 4, 1, and 1 μM, respectively (Fig. 3d, Supplementary Table 21 and Supplementary texts). Real-time atomic force microscopy (AFM) experiments confirmed that KDFA2i+9-NH2 (at a concentration ~1 μM) formed nanopores in the supported lipid bilayers composed of POPC:POPG (1:1 mol/mol) lipids and can cause significant bilayer disruption at higher concentrations (Fig. 3e, Supplementary Figs. 19-20 and Supplementary texts). Further, the cryo-EM micrographs indicated the formation of transmembrane peptide assemblies/pores in nanometer scale, although such small size and flexibility of the structures prevented their high-resolution determination (Supplementary Fig. 21). All these experimental data (AFM, cryo-EM, and vesicle leakage measurements) together with MD simulations consistently support the formation of TBPs and suggest the pore-forming mechanism of antibacterial action of our designed AMPs.

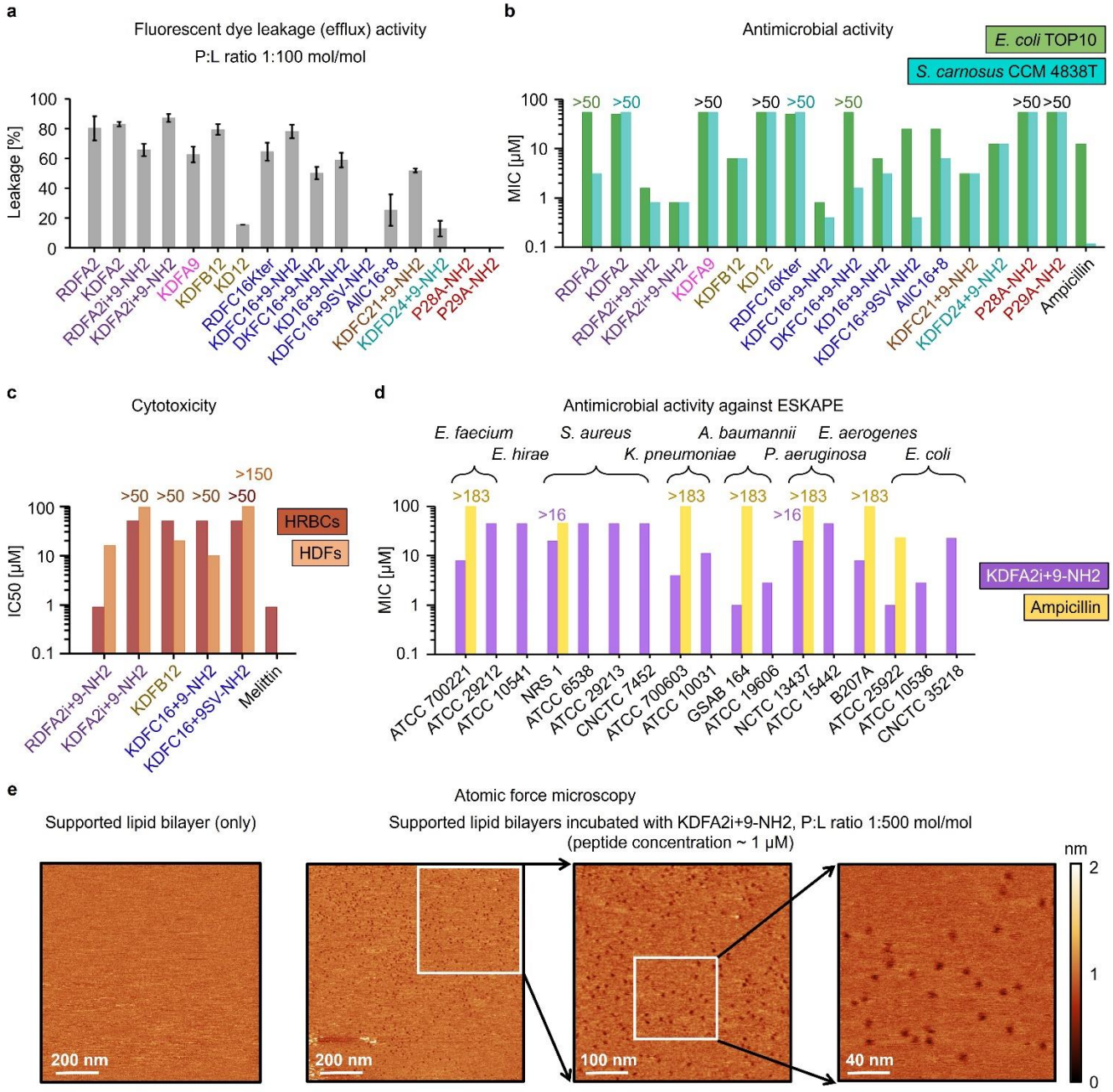

Fig. 3 | *In vitro* characterization of designed peptides. a, Peptide-induced leakage (efflux) of the fluorescent dye calcein from POPC:POPG (1:1 mol/mol) LUVs; **b,** peptide antimicrobial activity against Gram-negative *Escherichia coli* and Gram-positive *Staphylococcus carnosus* bacteria; **c,** peptide cytotoxicity against HRBCs and HDFs; **d,** peptide antimicrobial activity against the resistant ESKAPE pathogens; **e,** AFM topographic images of the supported lipid bilayers composed of POPC:POPG (1:1 mol/mol) lipids, before and after 1 hour incubation with KDFA2i+9-NH2 peptides, showing membrane nanopore formation.

In summary, we describe a computational approach and experimental validation process for the *de novo* design of nanometer-sized TBP-forming α-helical peptides. Our approach provides the molecular understanding of the relationship between peptide sequences and stability of TBPs. The identified role of individual residues in the proposed pore-forming sequence patterns facilitates the custom design of functional peptide nanopores for specific applications. We demonstrate such customization with fine-tuning of the sequences into potent pore-forming AMPs killing even antibiotic-resistant bacteria, while having low toxicity for human cells. Such peptides with high therapeutic index could be a good starting point for the development of next antibiotics. Similar customization can be performed for other medical and biotechnological applications, including anticancer agents[29], single-molecule sensing and sequencing[1,2].

References

1. Howorka, S. Building membrane nanopores. *Nat. Nanotechnol.* **12**, 619–630 (2017).
2. Majd, S. *et al.* Applications of biological pores in nanomedicine, sensing, and nanoelectronics. *Curr. Opin. Biotechnol.* **21**, 439–476 (2010).
3. Brogden, K. A. Antimicrobial peptides: pore formers or metabolic inhibitors in bacteria? *Nat. Rev. Microbiol.* **3**, 238–250 (2005).
4. Lazzaro, B. P., Zasloff, M. & Rolff, J. Antimicrobial peptides: Application informed by evolution. *Science* **368**, (2020).
5. Magana, M. *et al.* The value of antimicrobial peptides in the age of resistance. *Lancet Infect. Dis.* **20**, e216–e230 (2020).
6. Wang, G., Li, X. & Wang, Z. APD3: the antimicrobial peptide database as a tool for research and education. *Nucleic Acids Res.* **44**, D1087–D1093 (2016).
7. Tuerkova, A. *et al.* Effect of helical kink in antimicrobial peptides on membrane pore formation. *eLife* **9**, e47946 (2020).
8. Lear, J. D., Wasserman, Z. R. & Degrado, W. F. Synthetic amphiphilic peptide models for protein ion channels. *Science* **240**, 1177–1181 (1988).
9. Joh, N. H. *et al.* De novo design of a transmembrane Zn2+-transporting four-helix bundle. *Science* **346**, 1520–1524 (2014).
10. Lu, P. *et al.* Accurate computational design of multipass transmembrane proteins. *Science* **359**, 1042–1046 (2018).
11. Xu, C. *et al.* Computational design of transmembrane pores. *Nature* **585**, 129–134 (2020).
12. Scott, A. J. *et al.* Constructing ion channels from water-soluble α-helical barrels. *Nat. Chem.* **13**, 643–650 (2021).
13. Mahendran, K. R. *et al.* A monodisperse transmembrane α-helical peptide barrel. *Nat. Chem.* **9**, 411–419 (2017).
14. Krishnan R, S. *et al.* Autonomously assembled synthetic transmembrane peptide pore. *J. Am. Chem. Soc.* **141**, 2949–2959 (2019).
15. Mravic, M. *et al.* Packing of apolar side chains enables accurate design of highly stable membrane proteins. *Science* **363**, 1418–1423 (2019).
16. Guha, S., Ghimire, J., Wu, E. & Wimley, W. C. Mechanistic Landscape of Membrane-Permeabilizing Peptides. *Chem. Rev.* **119**, 6040–6085 (2019).
17. Ulmschneider, J. P. & Ulmschneider, M. B. Molecular Dynamics Simulations Are Redefining Our View of Peptides Interacting with Biological Membranes. *Acc. Chem. Res.* **51**, 1106–1116 (2018).
18. de Jong, D. H. *et al.* Improved Parameters for the Martini Coarse-Grained Protein Force Field. *J. Chem. Theory Comput.* **9**, 687–697 (2013).
19. Bowie, J. U. Helix packing in membrane proteins. *J. Mol. Biol.* **272**, 780–789 (1997).
20. Matsuzaki, K. Control of cell selectivity of antimicrobial peptides. *Biochim. Biophys. Acta BBA - Biomembr.* **1788**, 1687–1692 (2009).
21. Walther, T. H. & Ulrich, A. S. Transmembrane helix assembly and the role of salt bridges. *Curr. Opin. Struct. Biol.* **27**, 63–68 (2014).
22. Mani, R. *et al.* Membrane-dependent oligomeric structure and pore formation of a β-hairpin antimicrobial peptide in lipid bilayers from solid-state NMR. *Proc. Natl. Acad. Sci.* **103**, 16242–16247 (2006).
23. Fox, R. O. & Richards, F. M. A voltage-gated ion channel model inferred from the crystal structure of alamethicin at 1.5-Å resolution. *Nature* **300**, 325–330 (1982).
24. Dawson, J. P., Weinger, J. S. & Engelman, D. M. Motifs of serine and threonine can drive association of transmembrane helices. *J. Mol. Biol.* **316**, 799–805 (2002).
25. Meng, X., Li, T., Zhao, Y. & Wu, C. CXC-mediated cellular uptake of miniproteins: forsaking "arginine magic". *ACS Chem. Biol.* **13**, 3078–3086 (2018).
26. Yang, S.-T. *et al.* Selective cytotoxicity following Arg-to-Lys substitution in tritrpticin adopting a unique amphipathic turn structure. *FEBS Lett.* **540**, 229–233 (2003).
27. Yeaman, M. R. & Yount, N. Y. Mechanisms of antimicrobial peptide action and resistance. *Pharmacol. Rev.* **55**, 27–55 (2003).
28. Raghuraman, H. & Chattopadhyay, A. Melittin: a membrane-active peptide with diverse functions. *Biosci. Rep.* **27**, 189–223 (2007).
29. Gaspar, D., Veiga, A. S. & Castanho, M. A. From antimicrobial to anticancer peptides. A review. *Front. Microbiol.* **4**, 294 (2013).

Acknowledgements

We thank Martina Drabinová and Tereza Králová for help with experiments; Naďa Labajová for advice on SLB formation; Guy Riddihough for help with the manuscript writing; and Pavel Jungwirth for careful reading of the manuscript. We also thank the members of Vácha group for discussions.

Funding

The work was supported by the Czech Science Foundation (grant 20-20152S) and the Ministry of Education, Youths and Sports of the Czech Republic (project LL2007 under the ERC CZ program), and the European Research Council (ERC) under the European Union's Horizon 2020 research and innovation programme (grant agreement No 101001470). Additional support for experiments was provided by the project Development of the System of Commercialization of Results at Masaryk University TG02010067 financed by the Technology Agency of the Czech Republic. Computational resources were provided by the CESNET LM2015042 and the CERIT Scientific Cloud LM2015085 provided under the program Projects of Large Research, Development, and Innovations Infrastructures. For AFM and Cryo-EM experiments, we acknowledge CF Nanobiotechnology and CF Cryo-EM (CEMCOF) of CIISB, respectively, and Instruct-CZ Centre supported by MEYS CR (LM2018127).

Author contributions

R.D. and R.V. conceived the project and designed research. R.D. carried out MD simulations and analyzed data. I.K. contributed with technical solutions to the problems in simulations. R.D. and R.V. designed the peptides and developed the design guidelines. R.D. conducted vesicle leakage assay with help of I.K. R.D. and

I.K. carried out broth microdilution and hemolysis assays. R.D. and J.P. performed AFM experiments. R.D. analyzed experimental data with help of I.K. and J.P. R.D. and R.V. wrote the manuscript with comments from all the authors.

Competing interests

Authors R.D., I.K., and R.V. are inventors on a EU Patent application filed by Masaryk University that covers the peptides and design guidelines described in this paper.

Data and materials availability

All data needed to evaluate the conclusions in the paper are available in the main text or the supplementary materials.

Supplementary information

Methods
Supplementary texts
Supplementary Tables 1-22
Supplementary Figs. 1-22
References 30-6